A Two-Step Phase-Shifting Phase Retrieval Algorithm Based on Orthogonal Characteristics of Interfeograms

Jinping Fan(✉), Chunjun Li, Yingjie Cui, Xuemei Cao, and Jingdan Zhang

Electronic Communication Technology Department, Shenzhen Institute of Information Technology, Shenzhen 518172, China
fanjp@sziit.edu.cn

Abstract. A new two-step phase-shifting phase retrieval method is put forward to recover the real phase of the measured object through the orthogonal characteristics of the diamond diagonal vectors from three phase shift interference fringe patterns whose phase shifts are random and unknown. From the results of both simulation and experiment prove that the proposed method can obtain the phase to be measured with fast speed and high accuracy.

Keywords: Interferometry · Phase measurement · Phase shift · Phase retrieval

1 Introduction

As a high-precision optical measurement technology, optical phase-shifting interferometry has been used in scientific research and engineering applications broadly and deeply. Traditional phase-shifting phase retrieval method, which called N-step phase-shifting algorithm ($N \geq 3$), is to recover the measured phase by calculating N-frame of phase-shifting interferograms whose phase shift is the same or a fixed value (mostly 90°), such as equal-step algorithm and fixed-step algorithm [1]. These methods have high requirements on the value of phase shift, in order to obtain high-precision of phase information, such algorithms usually need to calibrate the phase shifter [2]. Obviously, the phase shift error is one of the main element affecting the precision of the traditional phase-shifting phase retrieval algorithm. For the needs of practical engineering applications, it is necessary to study the phase-shifting phase measurement method when the phase shift amount is unknown or random. In recent decades, multi-step phase retrieval algorithms whose phase shifts are random and unknown have been put forward, mainly include the advanced iterative algorithm (AIA) [3], the principal component analysis (PCA) [4], the Euclidean matrix norm (EMN) [5], etc. The above mentioned algorithms or method require at least three or more interferograms to perform effective caluations.

Two-step phase-shifting interferometry, which can retrieve the phase quickly and accurately from two phase-shifting interference fringe patterns whose phase shifts are random and unknown [6–12]. In a large range, approximately $0.16\pi \sim 0.45\pi$, the results aren't influenced by the value of the phase shift. This makes the airflow changes and vibration and many more environmental factors significantly reduced so that can be

M. Guan and Z. Na (Eds.): MLICOM 2020, LNICST 342, pp. 27–35, 2021.
https://doi.org/10.1007/978-3-030-66785-6_3

applied to dynamic phase measurement. However, for most two-step phase-shifting methods, it is necessary to remove the background items of the fringe patterns in advance. For interferograms with slowly changing background intensity, the background items can be eliminated with a filter in the frequency domain. However, for interferograms with high-frequency background intensity changes, although the method of filtering in the frequency domain can filter out the background part, the high-frequency phase information has also been filtered out. In addition, the choice of filter window size has a direct and important influence on the accuracy of the two-step algorithm. These will bring certain errors to the measurement results.

To resolve such problems, interferograms subtraction method is employed to remove background item, the phase to be measured can be obtained fast and accurately [13]. In this work, combined with the interferogram subtraction and the orthogonal characteristics of three phase-shifting interferograms, a new two-step phase-shifting phase retrieval method is proposed to reconstruct the measured phase rapidly and accurately. Next we will first introduce the principle of the proposed method, and then show the effectiveness of the proposed method through the numerical simulation and experimental research.

2 Principle

Generally speaking, for the m-th pixel of the n-th phase shift interference fringe pattern, the distribution of the intensity expressed as

$$I_{mn} = A_m + B_m \cos[\phi_m + \delta_n] \tag{1}$$

where n = 1, 2, 3 represent the serial number of the interference fringe patterns; m = 1, 2, …, M denote the position of the pixel, the sum of all pixels on the interferogram is M; $A_{m,}$ B_m and φ_m respectively denote the background item, modulation item and phase to be measured; δ_n represent the n-th interferogram phase shift of unknown and random. For simplicity, we define δ_1 = 0. Two frames of differential interference fringe patterns can be obtained through subtraction of the 2nd and 3rd interferograms from 1st interferogram which can be expressed as

$$D_{m1} = I_{m1} - I_{m2} = 2B_m \sin\frac{\delta_2}{2} \sin \Phi_m \tag{2}$$

$$D_{m2} = I_{m1} - I_{m3} = 2B_m \sin\frac{\delta_3}{2} \sin(\Phi_m + \Delta) \tag{3}$$

where $\Phi_m = \phi_m + \frac{\delta_2}{2}$, $\Delta = \frac{\delta_3 - \delta_2}{2}$. Through the plain subtraction operation, the background item A_m has been removed thoroughly. In practical phase-shifting interferometry, due to the different interference fringe patterns have different phase shifts, expressed as $B_m \sin\frac{\delta_2}{2} \neq B_m \sin\frac{\delta_3}{2}$, which make two differential interferograms have different amplitudes. In order to remove the phase shift influence on differential

interferograms amplitudes, normalization operation has been utilized. The normalized vector of u can be denoted as

$$\tilde{u} = \frac{u}{\sqrt{<u \cdot u>}} = \frac{u}{\|u\|} \tag{4}$$

where $<u \cdot u> = u^T u$, the superscript T stands for transpose operation. Normalizing Eqs. (2) and (3), we can obtain

$$\tilde{D}_{m1} = \frac{2B_m \sin\frac{\delta_2}{2} \sin \Phi_m}{2 \sin\frac{\delta_2}{2} \sqrt{\sum_{m=1}^{M} B_m^2 \sin^2 \Phi_m}} = \frac{B_m \sin \Phi_m}{\sqrt{\sum_{m=1}^{M} B_m^2 \sin^2 \Phi_m}} \tag{5}$$

$$\tilde{D}_{m2} = \frac{2B_m \sin\frac{\delta_3}{2} \sin(\Phi_m + \Delta)}{2 \sin\frac{\delta_3}{2} \sqrt{\sum_{m=1}^{M} B_m^2 \sin^2(\Phi_m + \Delta)}} = \frac{B_m \sin(\Phi_m + \Delta)}{\sqrt{\sum_{m=1}^{M} B_m^2 \sin^2(\Phi_m + \Delta)}} \tag{6}$$

If there are more than one fringe numbers in the interference fringe pattern, the following approximate expression can be obtained as

$$\sum_{m=1}^{M} B_m^2 \sin^2 \Phi_m - \sum_{m=1}^{M} B_m^2 \sin^2(\Phi_m + \Delta) = \sin(-\Delta) \sum_{m=1}^{M} B_m^2 \sin(2\Phi_m + \Delta) \approx 0 \tag{7}$$

And then we will get the following approximation

$$\sqrt{\sum_{m=1}^{M} B_m^2 \sin^2 \Phi_m} \approx \sqrt{\sum_{m=1}^{M} B_m^2 \sin^2(\Phi_m + \Delta)} \tag{8}$$

Rewrite Eqs. (5) and (6) we can get

$$\tilde{D}_{m1} = \frac{B_m \sin \Phi_m}{\sqrt{\sum_{m=1}^{M} B_m^2 \sin^2 \Phi_m}} = b_m \sin \Phi_m \tag{9}$$

$$\tilde{D}_{m2} = \frac{B_m \sin(\Phi_m + \Delta)}{\sqrt{\sum_{m=1}^{M} B_m^2 \sin^2(\Phi_m + \Delta)}} \approx b_m \sin(\Phi_m + \Delta) \tag{10}$$

where $b_m = \frac{B_m}{\sqrt{\sum_{m=1}^{M} B_m^2 \sin^2 \Phi_m}}$. It can be seen from the above two equations that the two differential interferograms has same amplitudes. We can obtain the following expression if the fringe number of the interferograms is more than one.

$$\left\|\tilde{D}_{m1}\right\| = \sqrt{\sum_{m=1}^{M} b_m^2 \sin^2 \Phi_m} \approx \left\|\tilde{D}_{m2}\right\| = \sqrt{\sum_{m=1}^{M} b_m^2 \sin^2(\Phi_m + \Delta)} \tag{11}$$

It can be seen that the lengths of $\tilde{D}_{m1}$ and $\tilde{D}_{m2}$ are approximately equal and they can be regard as equal-length vectors. According to the law of parallelograms of vectors, we can see that the sum and subtraction of the two equal-length vectors are the diagonal vectors of the diamond which formed by these two equal-length vectors, and these two diagonal vectors are orthogonal to each other. The two orthogonal diagonal vectors of the diamond can be expressed as

$$\tilde{d}_{m1} = \tilde{D}_{m2} - \tilde{D}_{m1} = 2b_m \sin\frac{\Delta}{2}\cos\psi_m \tag{12}$$

$$\tilde{d}_{m2} = \tilde{D}_{m2} + \tilde{D}_{m1} = 2b_m \cos\frac{\Delta}{2}\sin\psi_m \tag{13}$$

where $\psi_m = \Phi_m + \frac{\Delta}{2}$. Normalizing the two orthogonal diagonal vectors of formulas (12) and (13), we will get

$$\hat{d}_{m1} = \frac{\tilde{d}_{m1}}{\left\|\tilde{d}_{m1}\right\|} = \frac{2b_m \sin\frac{\Delta}{2}\cos\psi_m}{2\sin\frac{\Delta_i}{2}\sqrt{\sum_{m=1}^{M} b_m^2 \cos^2\psi_m}} = \frac{b_m \cos\psi_m}{\sqrt{\sum_{m=1}^{M} b_m^2 \cos^2\psi_m}} \tag{14}$$

$$\hat{d}_{m2} = \frac{\tilde{d}_{m2}}{\left\|\tilde{d}_{m2}\right\|} = \frac{2b_m \cos\frac{\Delta}{2}\sin\psi_m}{2\cos\frac{\Delta}{2}\sqrt{\sum_{m=1}^{M} b_m^2 \sin^2\psi_m}} = \frac{b_m \sin\psi_m}{\sqrt{\sum_{m=1}^{M} b_m^2 \sin^2\psi_m}} \tag{15}$$

Under the above assumption of more than one fringe numbers, we can get the following expression.

$$\sqrt{\sum_{m=1}^{M} b_m^2 \cos^2\psi_m} \approx \sqrt{\sum_{m=1}^{M} b_m^2 \sin^2\psi_m} \tag{16}$$

Though a simple arctangent operation we can get the measured phase.

$$\psi_m = \arctan\left(\frac{\hat{d}_{m2}}{\hat{d}_{m1}}\right) \tag{17}$$

3 Numerical Simulation

In order to prove the effectiveness of the proposed method, we conducted simulation verification. First of all, on the basis of formula (1), three simulated phase-shifting interference fringe patterns with size of 512 × 512 pixels are generated, the phase shifts are respectively set as $\delta_1 = 0$, $\delta_2 = 1$ and $\delta_3 = 2$. Among them, the background item is set as $A(x, y) = 10\exp[-0.2(x^2 + y^2)] = 80$, the modulation item is $B(x, y) = 80\exp[-0.25(x^2 + y^2)]$, where $-2.56 \leq x, y \leq 2.56$. The phase distribution to be measured is $\varphi(x, y) = \pi(x^2 + y^2) - < \pi(x^2 + y^2) >$ rad, where the operator $< \bullet >$ denote the average operation. In the simulated interferograms, an additive Gaussian noise with a signal-to-noise ratio of 5% has been added to achieve the actual situation.

Three simulated phase-shifting interferograms with a size of 512 × 512 pixels are shown in Figs. 1(a)–(c). Subtract Fig. 1(b) and 1(c) from Fig. 1(a), two differential

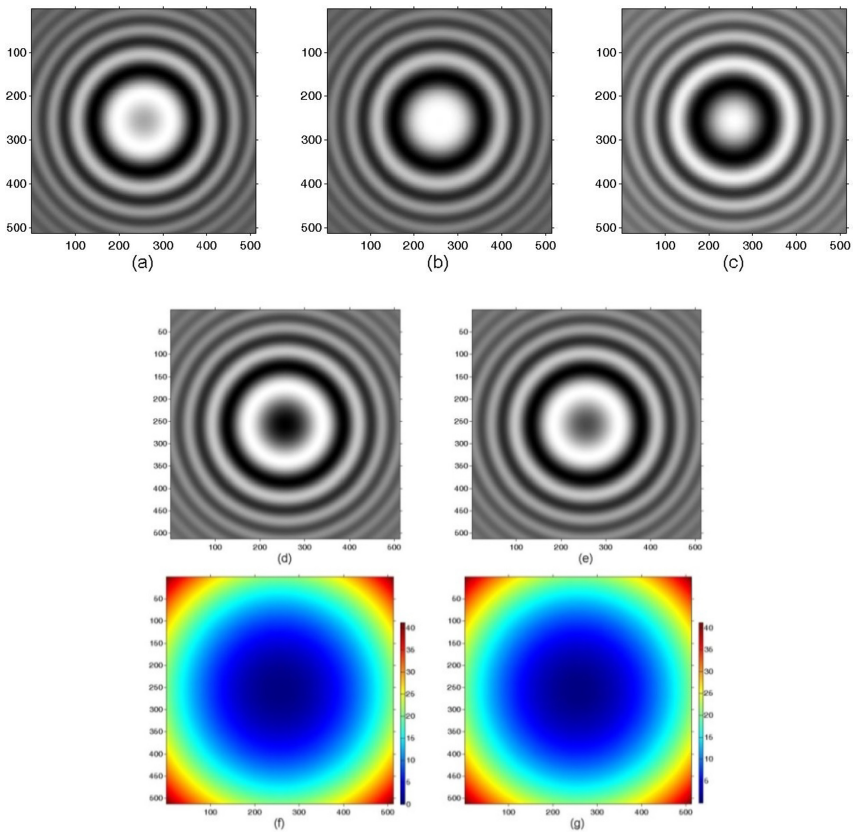

Fig. 1. Simulated phase-shifting interferograms. (a) (b) (c) three simulated phase-shifting interferograms; (d) (e) two differential interferograms; (f) the real phase; (g) the unwrapped phase of the proposed method.

interferograms shown in Fig. 1(d) and 1(e) can be obtained. Theoretical phase and unwrapped phase of the proposed method are shown in Fig. 1(f) and Fig. 1(g) respectively. Between the real phase and the measured phase, the root mean square error is measured as 0.0294 rad.

Next, AIA, PCA, GS3, DDV and GS2 have been utilized to compare with the phase measurement results of the proposed method, in which the numbers of fringe patterns are set as 32 for AIA and PCA, 3 for GS3, 2 for DDV and GS2. For AIA and PCA, the phase shift between two neighboring interferograms is set as 0.1 rad. Conventional Gaussian high-pass filter, whose transfer function expressed as $H(u, v) = 1\text{-}\exp[-(u^2 + v^2)/2\sigma^2]$, where σ represents filter window width and the value is 2, has been utilized to eliminate the background item in the algorithm of GS2 and DDV. Figure 2 (a)–2(f) show phase difference between the real phase and the unwrapped phase of AIA, PCA, GS2, DDV, GS3 and the proposed algorithm. To facilitate analysis and comparison, two important parameters, root mean square error (RMSE) and processing time, have been used to compare different methods as shown in Table 1. All results are obtained with a 2.5 GHz laptop and MATLAB.

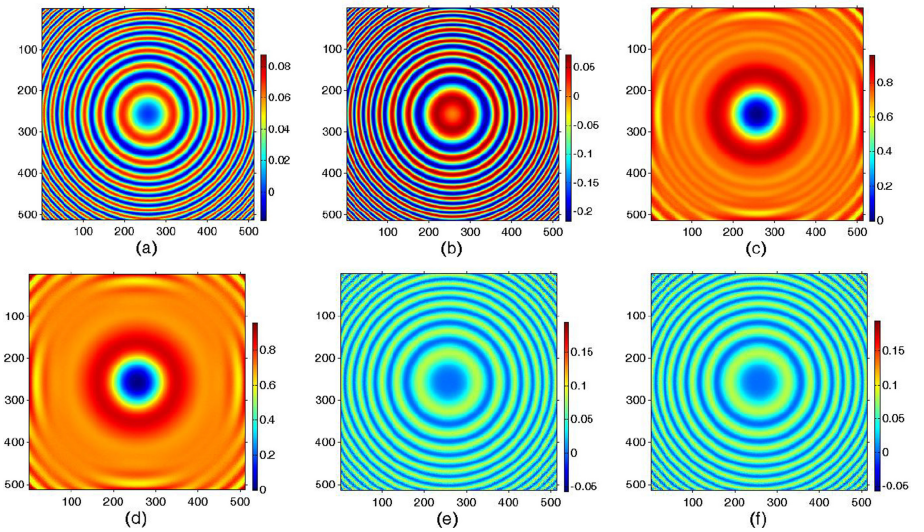

Fig. 2. The phase difference between the theoretical phase and the unwrapped phase with different algorithms: (a) AIA; (b) PCA; (c) GS2; (d) DDV; (e) GS3; (f) the proposed method

Obviously, the processing speed of the method proposed in this paper is lower than all other methods; in addition, the RMSE with the proposed method is the same with the GS3 and is close to AIA method with the longest processing time, and is far less than PCA, GS2 and DDV method. From the comparison result, the measurement accuracy of AIA is better than other methods. Therefore, in the experiment research, we use AIA measurement result as the reference phase.

Table 1. RMSE and the computing Time of different Algorithms (Simulation)

	AIA	PCA	GS2	DDV	GS3	The proposed method
RMSE (rad)	0.0281	0.0929	0.1085	0.1080	0.0294	0.0294
Time (s)	36.2890	0.4091	0.1683	0.0629	0.0258	0.0244

4 Experiment

Next, the effectiveness of the proposed method is verified by experiments research and the AIA measurement result is used as the reference phase. Three experimental interferograms selected randomly from 32-frame phase-shifting interferograms are shown in Fig. 3. Figure 4(a) shows the reference phase calculated by using AIA from 32-frame phase-shifting interferograms. Figures 4(b)–4(f) show the difference between

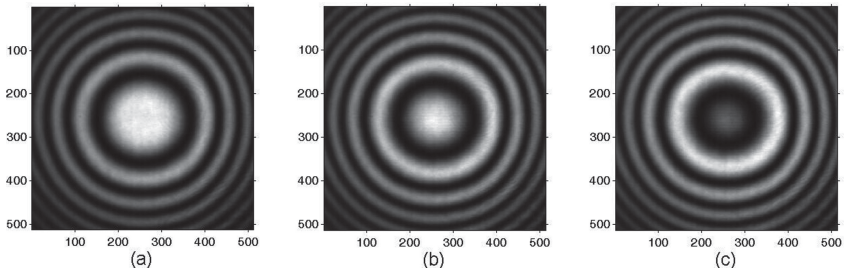

Fig. 3. Three-frame experimental phase-shifting interferograms

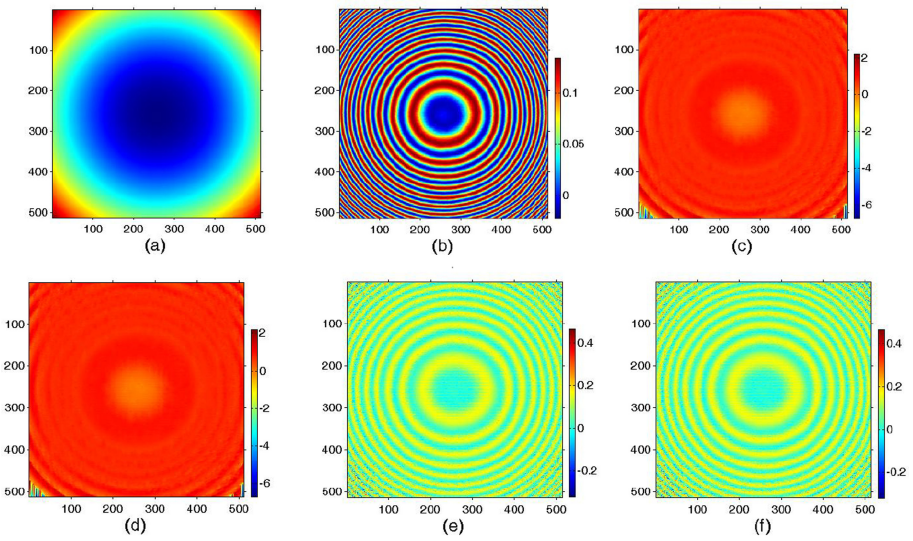

Fig. 4. The experimental results: (a) The referenced unwrapped phase of AIA; difference between the referenced AIA phase and the unwrapped phase of other methods: (b) PCA; (c) GS2; (d) DDV; (e) GS3; (f) the proposed method

the unwrapped phase maps of PCA, GS2, DDV, GS3 and the proposed method with the referenced phase map of AIA. The corresponding RMSE of the difference between referenced AIA and other methods, and the processing time are respectively shown in Table 2.

Table 2. RMSE and the processing Time of Phase Extraction with different Algorithms (Experiment)

	PCA	GS2	DDV	GS3	The proposed method
RMSE (rad)	0.0707	0.2829	0.2826	0.0625	0.0625
Time (s)	0.3450	0.0916	0.0646	0.0268	0.0252

It can be seen from the calculation results that the processing time of the proposed method in this paper is less than all other methods; in addition, the RMSE with the proposed method is the same with the GS3 and is close to the referenced AIA, and is far less than PCA, GS2 and DDV algorithm. The experimental results show that the proposed algorithm is suitable for the phase extraction with high precision and fast speed.

5 Conclusions

By using the interferogram subtraction and then normalization processing to remove the background, according to the orthogonal characteristics of the diamond diagonal vectors, only three phase-shifting interferograms whose phase shifts are unknown and randomly are needed to recover the real phase with high accuracy and fast speed. From the numerical simulation and experimental results, we can see that processing time of the method introduced in this paper is less than all other methods, in addition, the RMSE of the proposed method is the same with the GS3 and is close to AIA method with the longest processing time, and the result is far less than the PCA, GS2 and DDV algorithm. In summary, the algorithm proposed in this paper provides a very useful phase extraction tool.

Acknowledgements. This work is supported by the Natural Science Foundation of Guangdong (Grant No. 2017A030313337), Shenzhen Science and Technology Project (Grant No. JCYJ20190808093001772), the Development Program Funds of Shenzhen Institute of Technology (Grant No. ZY201704).

References

1. Malacara, D., Servín, M., Malacara, Z.: Interferogram analysis for optical testing. CRC Press (2005)
2. Creath, K.: Phase-measurement interferometry techniques. Prog. Opt. **26**(26), 349–393 (1988)

3. Wang, Z., Han, B.: Advanced iterative algorithm for phase extraction of randomly phase-shifted interferograms. Opt. Lett. **29**(14), 1671–1673 (2004)
4. Vargas, J., Quiroga, J.A., Belenguer, T.: Analysis of the principal component algorithm in phase-shifting interferometry. Opt. Lett. **36**(12), 2215–2217 (2011)
5. Deng, J., Wang, H., Zhang, D., Zhong, L., Fan, J., Lu, X.: Phase shift extraction algorithm based on euclidean matrix norm. Opt. Lett. **38**(9), 1506–1508 (2013)
6. Kreis, T.M., Jueptner, W.P.: Fourier transform evaluation of interference patterns: demodulation and sign ambiguity. In: Proceedings of Spiel the International Society for Optical Engineering, 1553 (1992)
7. Vargas, J., Quiroga, J.A., Sorzano, C.O.S., Estrada, J.C., Carazo, J.M.: Two-step interferometry by a regularized optical flow algorithm. Opt. Lett. **36**(17), 3485–3487 (2011)
8. Vargas, J., Quiroga, J.A., Sorzano, C.O.S., Estrada, J.C., Carazo, J.M.: Two-step demodulation on the Gram-Schmidt ortho normalization method. Opt. Lett. **37**(3), 443–445 (2012)
9. Muravsky, L., Ostash, O., Voronayk, T., et al.: Two-frame phase-shifting interferometry for retrieval of smoothy surface and its displacement. Opt. Lasers Eng. **49**(3), 305–132 (2011)
10. Deng, J., Wang, H., Zhang, F., et al.: Two-setp phase demodulation algorithm based on the extreme value of interference. Opt. Lett. **37**(3), 443–445 (2012)
11. Luo, C., Zhong, L., Sun, P., Wang, H., Tian, J., Lu, X.: Two-step demodulation algorithm based on the orthogonality of diamond diagonal vectors. Appl. Phys. B **119**(2), 387–391 (2015). https://doi.org/10.1007/s00340-015-6087-z
12. Niu, W., Zhong, L., Sun, P., Zhang, W.: Two-step phase retrieval algorithm based on the quotient of inner products of phase-shifting interferograms. J. Opt. **17**(8), 085703 (2015)
13. Wang, H., Luo, C., Zhong, L., Ma, S., Lu, X.: Phase retrieval approach based on the normalized difference maps induced by three interferograms with unknown phase shifts. Opt. Express **22**(5), 5147–5154 (2014)